한국기계가공학회지, 제17권, 제6호, pp.53～60(2018.12) ISSN 1598-6721(Print)
Journal of the Korean Society of Manufacturing Process Engineers, Vol. 17, No. 6, pp.53~60(2018.12) ISSN 2288-0771(Online)

https://doi.org/10.14775/ksmpe.2018.17.6.053

Study on Electrical Characteristics of FDM Conductive 3D Printing According to Annealing Conditions

Sun Kon Lee*, Yong Rae Kim*, Tae Jung Yoo*, Ji Hye Park*, Joo Hyung Kim*,#

*Department of Mechanical Engineering, Inha University

FDM 전도성 3D프린팅 어닐링 조건 따른 전기적 특성 연구

이선곤*, 김용래*, 유태정*, 박지혜*, 김주형*,#

*인하대학교 기계공학과

(Received 27 May 2018; received in revised form 22 June 2018; accepted 16 August 2018)

ABSTRACT

In this paper, the effect of different 3D printing parameters including laminated angle and annealing temperature is observed their effect on FDM conductive 3D printing. In FDM 3D printing, a conductive filament is heated quickly, extruded, and then cooled rapidly. FDM 3D Print conductive filament is a poor heat conductor, it heats and cools unevenly causing the rapid heating and cooling to create internal stress. when the printed conductive specimens this internal stress can be increase electrical resistance and decrease electrical conductivity. Therefore, This experiment would like to use annealing to remove internal stress and increase electrical conductivity. The result of experiment when 3D printing conductive specimen be oven cooling of annealing temperature 120℃ electrical resistance appeared decrease than before annealing. So We have found that 3D printing annealing removes internal stresses and increases the electrical conductivity of printed specimens. These results are very useful for making conductive 3D printing electronic circuit, sensor ect...with electrical conductance suitable for the application.

Key Words : Additive Manufacturing(적층가공), Conductive 3D Printing(전도성 3D프린팅), 3D printing Laminated Angle(3D프린팅 적층 각도), Conductive Annealing(전도성 어닐링)

1. Introduction

The three-dimensional (3D) printer is an additive manufacturing (AM) device that produces a shape by layer-by-layer deposition of materials rather than subtractive manufacturing, which produces a shape by cutting materials. 3D printing technology started from the rapid prototyping (RP) concept, but is now utilized in manufacturing of various products directly based on recent technological development[1,2,8].

This study is about optimization of conductive 3D printing using fused deposition modeling (FDM) 3D printers that have been widely utilized in various fields. To do this, this study investigated changes in electrical characteristics after resistance change and annealing in the 3D printing conductive specimens according to changes in lamination angle

Corresponding Author : joohyung.kim@inha.ac.kr
Tel: +82-32-860-7320, Fax: +82-32-868-6430

and the number of layers. This was done to identify the optimum printing conditions to improve electrical conductance so that the utilization of 3D printing can be expanded to various electrical and electronic application fields such as electronic circuits, flexible sensors, and capacitive sensors.

2. Experiment and discussion

This study measures electrical characteristics after printing conductive specimens by layer height according to the XY-angle of lamination using FDM conductive 3D printing; it compares and analyzes the changes in each of the electrical characteristics after annealing the specimen via constant-temperature oven. The basic concept of the conductive filament 3D printing is shown in Fig. 1. The FDM conductive 3D printing filament used in this experiment is a proto-pasta conductive PLA, which is a compound of Natureworks 4043D PLA, a dispersant and conductive carbon black.

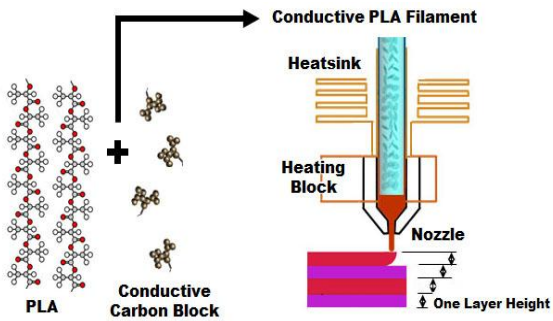

Fig. 1 Simplified schematics depicting the process of conductive PLA-based 3D printing using the technique of FDM

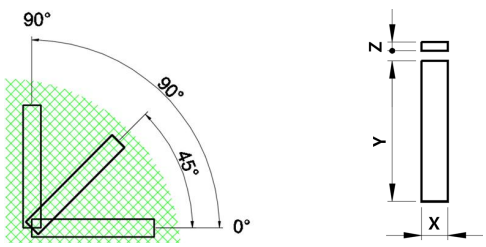

(a) XY-Angle **(b) Specimens design**

Fig. 2 Lamination XY-Angle and size of the conductive 3D printing specimens

Fig. 2 shows the definition of lamination of XY angles 0° and 45° and the specimen size. This study aims to investigate the effect on resistance characteristics of lamination angle and annealing on 3D printing conductive specimens while increasing the specimen size by 0.3-mm increments in the Z direction of the specimen, whose X and Y dimensions are 10 mm x 80 mm. Table 1 presents the 3D printing setup of the conductive specimen[3].

Both ends of the specimen were coated with silver paste (ELCOAT P-100, CANS), and a wire was connected as shown in Fig. 3 to measure the electrical characteristics of the 3D printing conductive specimen. Then, the specimen was fixed with non-conductive epoxy (S-209, ITW DEVCON), and the resistance characteristics of the conductive specimen were measured according to the 3D printing variables using a digital multimeter (34410a. Agilent). During FDM 3D printing, the amorphous structureless filament is restructured with large crystals (grains) through quenching immediately after high-temperature nozzle extrusion of the filament. Here, the line between the grains of the large crystals causes the weakening of the binding force. In addition, molecular orientation occurs due to the movements of printing nozzle, as well as difference in cooling speed between the surface and inside when the laminated structure via the extrusion of high-temperature filament is cooled. This study aims to analyze the effect of the structural defect of FDM 3D printing output on conductivity and to investigate the effect of annealing on electrical conductivity[4,5,6]. The glass transition temperature (Tg) and crystallization temperature of the conductive PLA filament were measured using a differential scanning calorimeter (DSC) to set up a

temperature for annealing. The measurement equipment used was DSC200F3, manufactured by NETZSCH. The measurement results are shown in Fig. 3, in which PLA and carbon black's glass transition temperatures are approximately 62℃ and 880℃, respectively, and the crystallization temperature is approximately 120℃. Thus, the annealing temperature was set to 62℃, which was the glass transition temperature, and 120℃, which was the crystallization temperature.

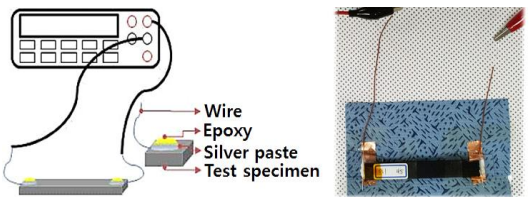

Fig. 3 Electrical Characteristic Evaluation Schematic

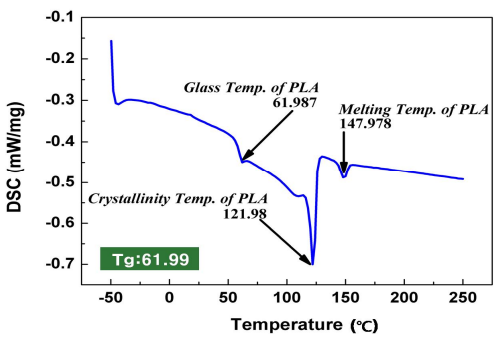

(a) PLA

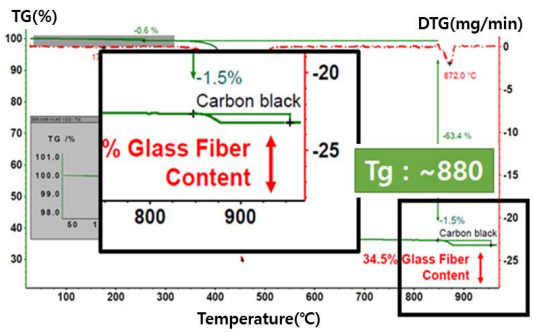

(b) Carbon black

Fig. 4 Glass transition temperature of conductive PLA Filament

Table 1 3D printer conditions

PC Condition	Value
Filament Diameter	1.75 (mm)
Nozzle Size	0.4 (mm)
Wall Thickness	0 (mm)
Bottom/Top Thickness	0 (mm)
Fill Density	100(%)
Print Speed	45 (mm/s)
Printing Temperature	220(℃)
Bed Temperature	40(℃)

2.1 Comparison of electrical characteristics of conductive specimens according to lamination angle and the number of layers

The layer height of the 10(X)×80(Y) mm specimen was fixed to 0.3 mm, and the number of layers was increased as presented in Table 2 to measure the changes in electrical resistance by lamination of XY angles of 0° and 45°.

Generally, since the polymer in the injection process is oriented in the resin flow direction, a difference in shrinkage ratio occurs between the flow and perpendicular directions. By this phenomenon, this study can predict that when the extrusion lamination direction, which is made by the movement of the high-temperature nozzle during 3D printing, is seen in the resin flow of the injection, the level of deformation in 3D printing objects will differ according to the lamination angle. Fig. 5 shows the schematic diagram of the 3D printing specimen in the orientation and shrinkage directions, in which the orientation of the XY-45° specimen is relatively longer in the Y-axis direction so that shrinkage in the Y-axis direction is larger than that of the XY-0° specimen. Furthermore, a phenomenon to compensate the shrinkage in the X-axis direction, which is perpendicular to the orientation, occurs such that the area becomes larger, and thus has a larger electrical resistance in XY-45° specimen.

Table 2 Conductive 3D printing specific size

X×Y×Z (mm)	layer Q'ty (EA)	X×Y×Z (mm)	layer Q'ty (EA)
10×80×0.3	1	10×80×3.0	10
10×80×0.6	2	10×80×3.3	11
10×80×0.9	3	10×80×3.6	12
10×80×1.2	4	10×80×3.9	13
10×80×1.5	5	10×80×4.2	14
10×80×1.8	6	10×80×4.5	15
10×80×2.1	7	10×80×4.8	16
10×80×2.4	8	10×80×6.0	20
10×80×2.7	9	10×80×12	40

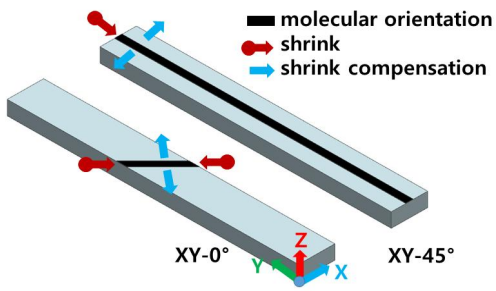

Fig. 5 Resistance curve for Lamination of XY-Angle

Fig. 6 shows of the measured changes in electrical resistance. Since the resistance is reduced if the area increases, the resistance will be reduced as the number of layers increases according to Eq. ①. The resistance measurement results show that when one layer was used, the resistances of XY-0° and -45° were 3,071Ω and 4,790Ω, respectively, which were very high, showing large difference in resistance according to a lamination angle, of 1,719 Ω. Thus, as the number of layers increased, deviation according to lamination angle was reduced, resulting in deviation smaller than 20Ω from 12 layers. This indicated that the effect of the lamination angle was minimal. The above results imply that although the lamination angle affected the resistance, the effect was minimal after the thickness of the lamination, which represents the number of layers, was approximately 3.6 mm or thicker.

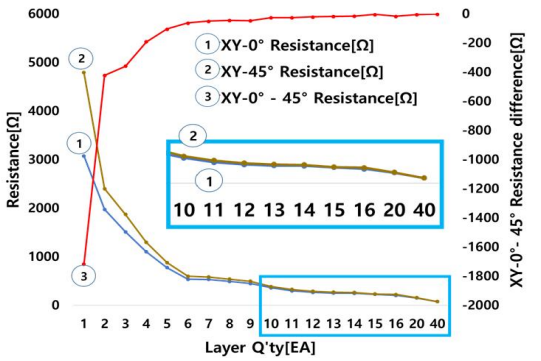

Fig. 6 Resistance curve for Lamination of XY-Angle

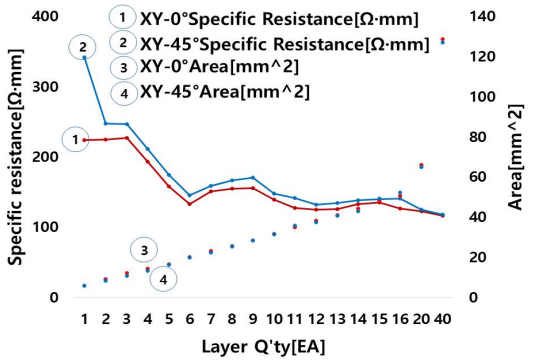

Fig. 7 Specific resistance curve and Area for Lamination of XY-Angle

For the specimen that had the smallest number of the layers, the effect of orientation in the XY-45° specimen was large so that a significant difference in shrinkage between the flow and perpendicular directions occurred, entailing a large electrical resistance due to the generated non-uniform crystal grains.

$$R = \rho\frac{L}{A}, \quad \rho = \frac{AR}{L} \cdots\cdots\cdots\cdots\cdots\cdots\cdots\cdots \quad ①$$

R : electrical resistance (Ω),

ρ : specific resistance(Ω·mm)

L : specimen length(mm),

A specimen's cross-section area (mm^2)

$$\sigma = \frac{1}{R} \cdots\cdots\cdots\cdots\cdots\cdots\cdots\cdots\cdots\cdots\cdots\cdots\cdots\cdots \quad ②$$

σ : electrical conductivity(1/Ω)

Fig. 7 shows the differences in specific resistance and area according to lamination angle, in which specific resistance is large at XY-45° and the difference in specific resistance is reduced as the number of layers increases.

The electrical conductivity represents the level at which the specimen can deliver the current, which can be expressed by an inverse of electrical resistance, as presented in Eq. ②.

At a 0.3-mm layer height, as the number of layers is smaller, electrical conductivity at XY-0° was better than that at XY-45°, but similar conductivity was exhibited at 12 layers or more, regardless of the lamination angle.

2.2 Comparison of annealing characteristics of conductive specimens according to lamination angle and the number of layers

The progress of annealing can be divided into three phases: recovery, recrystallization, and grain growth. In the recovery phase, atom diffusion occurs actively due to high-temperature thermal treatment. As a result, the strain energy stored in the inside is removed due to the dislocation movement. Here, the vacancy is reduced, and electrical conductivity is improved by eliminating dislocation, which is an unstable defect in terms of energy. In the recrystallization phase, after dislocation density is raised due to printing, grains with low dislocation density are generated, inducing grain refinement. After recrystallization is complete, the growth of grain boundary continues by slow cooling of the specimen so that grain coarsening occurs in the grain growth phase[7,8].

To measure the electrical characteristics due to annealing, layer height was set to 0.3 mm, and the number of layers was increased to increase the thickness (Z) in 0.3-mm increments. Printed 10(X)×80(Y)mm conductive specimens were then heat-applied in a constant-temperature oven at 62℃ and 120℃ (PLA glass transition temperature and crystallization temperature, respectively) for two hours. This was followed by oven cooling (cooling at a room temperature in the constant-temperature oven) to compare the electrical characteristics of the specimens before and after annealing.

Fig. 8 shows the annealing effects on XY-0° specimens. Electrical resistance in the specimen after annealing at 62℃ was significantly increased at a single-layer height, and the deviation was reduced as the number of layers increased. However, the electrical conductivity was not improved compared to that before annealing. Thus, this result indicated that annealing at 62℃ (the glass transition temperature) did not affect electrical conductivity.

Electrical resistance measurement of the specimen after annealing at 120℃ showed that the annealing effect increased as the number of layers decreased. Although the annealing effect was gradually decreased as the number of layers increased, the electrical conductivity was improved overall due to the annealing. The annealing effect was decreased with the increase in thickness of the specimen because of the larger heat energy required for grain refinement and equalization by annealing as the specimen became thicker due to the increase in the number of layers. This meant that the annealing temperature for improvements of electrical conductivity differed depending on the specimen size. Fig. 9 shows the annealing effect of XY-45° specimen, which is large at 120℃, as shown in the XY-0° specimen. Fig. 10 shows the change effect of electrical resistance due to annealing by lamination angle and temperature, in which the effects of reduction in electrical resistance and improvement of electrical conductivity due to annealing are large at XY-45° and 120℃.

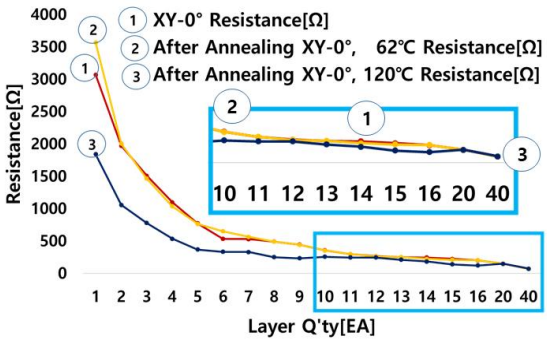

Fig. 8 Resistance curve for Lamination of XY-0° using oven cooling

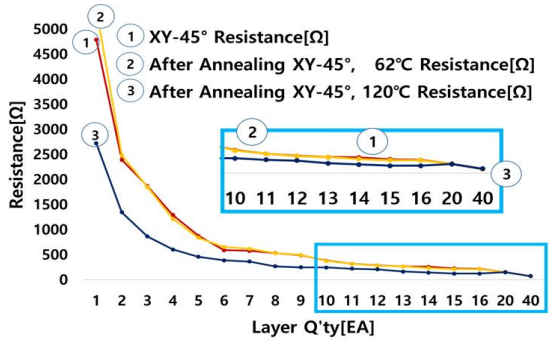

Fig. 9 Resistance curve for Lamination of XY-45° using oven cooling

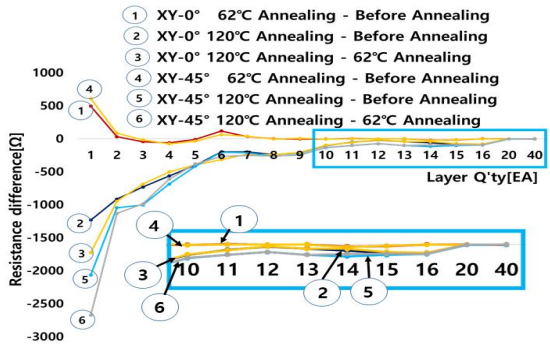

Fig. 10 Resistance different curve for Lamination of XY-Angle and Annealing temperature

This indicates that the non-uniformity of the specimen due to the internal stress occurred during 3D printing was large at XY-45°, which is why the grain refinement and equalization after annealing were large.

This experiment result revealed that the electrical conductivity of conductive 3D printing was improved by annealing.

3. Review and discussion

This study investigated the effect of annealing on electrical conductivity. The cause of the change in conductivity is a difference in mobility according to microstructure and temperature. Electrons are scattered in crystals; scattering by lattice vibration is due to the effect of nozzle temperature during printing, and the scattering degree increases as temperature increases. In addition, the defects of the microstructure such as impurity, precipitation, and dislocation influence the conductivity as well.

The effect of heat and microstructure on electrical resistance can be easily classified using Matthiessen's rule. Eq. ③ represents Matthiessen's rule, which is an empirical law to calculate the entire electrical resistance using the fact that electrons are scattered due to lattice defects or vibration. Here, the entire electrical resistance is equivalent to the sum of resistances due to each scattering. Thus, heat treatment due to annealing can improve electrical conductivity by removing the microstructure defects.

$$\rho_{Total} = \rho_{phonon} + \rho_{impurity} \quad \cdots\cdots\cdots\cdots\cdots\cdots \quad ③$$

ρ_{phonon} : phonon scattering

$\rho_{impurity}$: impurity scattering

The conductive filament during the conductive 3D printing process experiences deformation as it is passed through high-temperature melting and rapid cooling process. This deformation incurred damage to

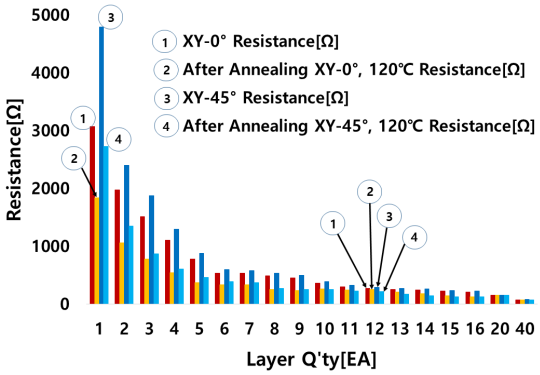

Fig. 11 Resistance curve for Lamination of XY-Angle and Annealing temperature

conductivity, which was then improved as the printing laminated object was stabilized through annealing.

Fig. 11 shows the changes in electrical resistance of the specimens before and after annealing at 120℃ by lamination angle, in which the resistance was lower after annealing regardless of lamination angle. This result indicated that the structural defects due to high-temperature extrusion and rapid cooling in FDM 3D printing affected conductivity, which was then improved by annealing.

The experiment results show that the electrical resistance of the conductive 3D printing laminated object was affected by the residual stress. The cause of residual stress generation that occurred during FDM 3D printing was that the melted filament during 3D printing attempted to be arranged to the stabilized state with polymer chain, but solidification occurred prior to stabilization, thereby generating residual stress in the printing structure. This phenomenon occurs due to the rapid cooling immediately after the melting filament is extruded at the nozzle. In addition, shear flow was generated due to the friction and cooling at the nozzle wall as a result of high-temperature extrusion and rapid cooling of the filament; consequently, that the extrusion speed was slower than that in the center of the nozzle, which was not affected by the shear. Thus, the outside of the melting filament during printing had higher shear stress than that in the inside due to higher shear strain thereby generating the residual stress. The defects due to the residual stress resulted in the increase in electrical resistance. Thus, electrical conductivity could be improved as a result of grain structure refinement, evenness, and grain growth by performing annealing to improve electrical conductivity and reduce the cause of residual stress.

4. Conclusions

The study results showed that the FDM 3D printing of a laminated object, which was a polymer structure, had energy that enabled movement and extension of molecular chains due to annealing, and this energy relaxed the internal stress due to non-uniform rapid cooling, thereby increasing grain refinement, equalization, and crystallization, resulting in improvements to electrical conductivity.

The electrical resistances of the specimen at XY 0° and 45° lamination angles, with 0.3-mm layer height and one layer, were 3,071Ω and 4,790Ω, but were reduced to 1,840Ω and 2,725Ω after annealing. This meant that the high electrical conductivity, which was the drawback of FDM conductive 3D printing, was improved by 40.1% and 43.1%, respectively, using annealing without structural changes or additional coating. In addition, the electrical resistances at 10 layers with 0° and 45° lamination angles were 357Ω and 383Ω, respectively, which showed that resistance at 45° was larger; however, the resistances after 120℃ annealing were 256Ω and 247.5Ω, respectively, which revealed that resistance at 0° was larger. This meant that as the specimen thickness increased, the internal stress at the 45° specimen had higher effect of grain refinement and evenness due to annealing.

The above study results indicate that electrical resistance can be controlled using lamination angle and annealing in conductive 3D printing, which not only contributes to the improvements of electrical conductivity in conductive 3D printing structures, but also identifies important factors in the development of various 3D printing sensors by controlling resistance.

Acknowledgment

This paper was supported by the Institute for Information and Communications Technology Promotion through funding from the Ministry of Science and ICT (No.2016-0-00 452, Development of creative technology based on complex 3D printing technology for labor, the elderly, and the disabled), and the Bio & Medical Technology Development Program of the National Research Foundation of Korea funded by the Ministry of Science and ICT (NRF-2017M3A9E2063256).

REFERENCES

1. Choi, J. W., Kim, H. C., "3D Printing Technologies - A Review," Journal of the Korean Society of Manufacturing Process Engineers, Vol. 14, No. 3, pp. 1~8, 2015.
2. Jang, J., Cho, D. W., “A Review of the Fabrication of Soft Structures with Three-dimensional Printing Technology,” Journal of the Korean Society of Manufacturing Process Engineers, Vol. 14, No. 6, pp. 142~148, 2015.
3. Kim, D. B., Lee, G. T., Lee, I. H., Cho, H. Y., “Finite Element Analysis for Fracture Criterion of PolyJet Materials,” Journal of the Korean Society of Manufacturing Process Engineers, Vol. 14, No. 4, pp. 134~139, 2015.
4. Lanzotti, A., Grasso, M., Staiano, G., Martorelli, M., “The impact of process parameters on mechanical properties of parts fabricated in PLA with an open-source 3-D printer,” Rapid Prototyping Journal, Vol. 21, No. 5, pp. 604-617, 2015.
5. Hashima, K., Nishitsuji, S., Inoue, T., “Structure-properties of super-tough PLA alloy with excellent heat resistance,” Polymer, Vol. 51, No. 17, pp. 3934-3939, 2010.
6. Postiglione, Giovanni., Natale, Gabriele., Griffini, Gianmarco., Levi, Marinella., Turri, Stefano., "Conductive 3D microstructures by direct 3D printing of polymer/carbon nanotube nanocomposites via liquid deposition modeling,” composites Part A, Vol. 76, pp. 110~114, 2015.
7. Seol, K. S., Shin, B. C., Zhang, S. U., "Fatigue Test of 3D-printed ABS Parts Fabricated by Fused Deposition Modeling," Journal of the Korean Society of Manufacturing Process Engineers, Vol. 17, No. 3, pp. 93~101, 2018.
8. Lee, S. K., Kim, Y. R., Kim, S. H., Kim, J, H., “Investigation of the Internal Stress Relaxation in FDM 3D Printing : Annealing Conditions,” Journal of the Korean Society of Manufacturing Process Engineers, Vol. 17, No. 4, pp. 130~136, 2018.